Chemical Engineering Journal 505 (2025) 159193

Contents lists available at ScienceDirect

Chemical Engineering Journal

journal homepage: www.elsevier.com/locate/cej

Highly efficient CO_2 capture from open air and dilute gas streams by tunable azolate ionic liquids based deep eutectic solvents

Guokai Cui [a,*], Yepin Cheng [a], Wei Zhang [b], Xiangyu Shen [a], Lai Li [b], Ruina Zhang [a], Yaoji Chen [b], Quanli Ke [a], Chunliang Ge [b], Huayan Liu [a], Wenyang Fan [b], Hanfeng Lu [a,*]

[a] *Innovation Team of Air Pollution Control, Institute of Catalytic Reaction Engineering, Zhejiang Key Laboratory of Surface and Interface Science and Engineering for Catalysts, State Key Laboratory Breeding Base of Green Chemistry Synthesis Technology, College of Chemical Engineering, Zhejiang University of Technology, Hangzhou 310014, China*

[b] *Zhejiang Zheneng Technology & Environment Group Co., Ltd., Hangzhou 310012, China*

ARTICLE INFO

Keywords:
Direct air capture
Deep eutectic solvent
CO_2 separation
Azolate ionic liquids
Cooperation

ABSTRACT

A series of functional deep eutectic solvents (DESs) forming from azolate ionic liquids (ILs) and ethylene glycol (EG) or succinonitrile (SN) were designed and synthesized for CO_2 capture with ultra-high uptake from open air (420–430 ppm) or dilute gas streams (500 ppm–5 vol%). With the increase of pKa of azoles, the CO_2 capacity of these azolate-based DESs increased linearly with $R^2 = 0.96$. Compared with other DESs and ILs, the extremely high CO_2 capture capacities of 14 wt% (3.18 mmol/g), 25 wt% (5.68 mmol/g), and 26 wt% (5.91 mmol/g) could be reached under open air / 500 ppm, 2 vol%, and 5 vol% CO_2, respectively, *via* tuning the structures of DESs. In addition, spectroscopic investigations revealed that the anion-induced multi-site cooperations of O···CO_2 and N···CO_2 were the reason of ultrahigh CO_2 capacities. To the best of our knowledge, these are the first examples of tuning amine-free functional DESs for the highly efficient CO_2 capture from open air. The significant improvements made in this work on CO_2 capture over conventional sorbents provide an alternative strategy for industrial gas capture and utilization *via* anion-induced multi-site cooperations.

1. Introduction

The increase concentration of CO_2 in the open air has been associated with global climate change and gives rise to direct air capture (DAC) technology.[1,2] Moreover, before the raw natural gas goes into pipeline, CO_2 concentration must be decreased below 2 % by carbon capture technologies to meet the US and most countries' pipeline standards to prevent corrosion and damage to equipment.[3] It is known that physical sorption and cryogenic separation can be applied for gas streams with higher CO_2 concentrations (typically > 50 %), while chemical sorption should be used for gas streams with lower CO_2 concentrations.[4,5] Conventional amine-based sorbents have been proved for efficient CO_2 capture for low-concentration CO_2 through chemical absorption. However, this technology results in high energy-consumption and high solvent-loss, as well as corrosion.[6] Thus, the designing and development of other highly efficient amine-free CO_2-philic sorbents for CO_2 capture and separation from open air (420–430 ppm) or dilute gas streams (500 ppm–5 vol%) is necessary but challenging.

Composed of cations and anions, ionic liquids (ILs) have been used as absorbents for the capture and separation of SO_2,[7–11] NO_x,[12–14] NH_3,[15–17] CO,[18–20] and especially CO_2,[21–26] *etc*. during these two decades due to their unique properties, including nonflammable, high thermo-stability, structural designability, *etc*.[27–31] However, the high viscosity limits the use of ILs for CO_2 in industry. For example, a saturated absorption capacity of 27 wt% CO_2 (6.1 mmol g^{-1}) could be achieved by neat amine-functional IL 1-hydroxyethyl-3-methylimidazolium lysine ([C_2OHmim][Lys]) after 60 h under 1 bar, with the state of IL changed from liquid to solid because of the strong chemical reactions.[32] In view of this, to avoid the effect of liquid viscosity on the liquid phase mass transfer, deep eutectic solvents (DESs),[33–35] composed of hydrogen bond accepters (HBAs) and hydrogen bond donors (HBDs), have been developed for CO_2 capture as the alternative sorbents with the similar tunable physical–chemical properties as the ILs.[21,36] For example, Zhang *et al.*[37] reported a series of amine-functionalized DESs for CO_2 capture with 1-butyl-3-methylimidazolium chloride ([Bmim][Cl]) as the HBA and monoethanolamine (MEA) as the HBD (molar ratios 1:1, 1:2 and 1:4), and the CO_2 capacities of these DESs were 8.4, 17.9, and 21.4 wt%, respectively, at 25 °C and 1 bar, indicating the

* Corresponding authors.
E-mail addresses: chemcgk@163.com (G. Cui), luhf@zjut.edu.cn (H. Lu).

https://doi.org/10.1016/j.cej.2024.159193
Received 28 September 2024; Received in revised form 5 December 2024; Accepted 31 December 2024
Available online 3 January 2025

larger the concentration of MEA, the higher the CO_2 absorption capacity. However, these DESs will result in the problem of conventional amine-based sorbents. Ren *et al.*[38] showed that the CO_2 capacities of functional DES based on triethylenetetramine hydrochloride ([TETAH][Cl]) as the HBA and thymol (Thy) as the HBD with the molar ratio of 1:3 were 9 % and 4.1 % at 40 °C under 1 bar and 0.1 bar, respectively. However, the desorptions of N–CO_2 carbamates formed *via* the reactions of amines and CO_2 always need more than 100°C to release CO_2 and obtain DESs. Besides, the viscosity of these functional DESs were dramatically increased after CO_2 absorption. For example, the viscosities of [TETAH][Cl]:Thy (1:3) and CO_2-saturated [TETAH][Cl]:Thy (1:3) were 205.1 and 6.77 × 10^3 mPa s, respectively.[38] Because of the azolate anion-functionalized ILs (AILs) could be used for efficient CO_2 capture as well as the high CO_2 absorption capacity and low absorption enthalpy of 1,2,4-triazolate ILs, [39–42] Yang *et al.*[43] reported that the CO_2 absorption capacities of DESs with 1,2,4-triazolate IL-based HBAs and ethylene glycol (EG) HBA were around 12 % at 25 °C and 1 bar, as well as the completely desorption could be achieved at 70 °C under 1 bar N_2. Although some AIL-based DESs have been developed for CO_2 capture, the CO_2 absorption capacities were still low and the data were limited, especially for CO_2 capture from open air or dilute gas streams.[44–47] Thus, novel sorbents with highly efficient capture of CO_2 from open air and dilute gas streams are highly desired.

Herein, we designed and synthesized a series of amine-free AIL-based DESs. These DESs are AILs as the HBAs as well as EG and succinonitrile (SN) as the HBDs with the molar ratio of HBA:HBD = 2:1, 1:1 and 1:2, and the structure of these DESs can be found in Fig. 1. With adjusting the structures of DESs and considering the physical and chemical properties, CO_2 capture by the functional DES formed with 1,5-diazabicyclo[4.3.0]non-5-enium pyrazolate ([DBNH][Pyrz]) as the HBA and EG as the HBD with molar ratio of HBA:HBD = 1:1 exhibited an ultrahigh CO_2 capture capacities of 14 wt% (3.18 mmol g^{-1}), 25 wt% (5.68 mmol g^{-1}), and 26 wt% (5.91 mmol g^{-1}) under open air / 500 ppm, 2 vol%, and 5 vol% CO_2, respectively. To the best of our knowledge, these capacities are superior than that of other DESs and ILs. Spectroscopic investigations revealed that the anion-induced multi-site cooperations of O···CO_2 and N···CO_2 were the reason of ultrahigh CO_2 capacities.

2. Experimental methods

2.1. Materials

1,5-Diazabicyclo[4.3.0]non-5-ene (DBN, 98 wt%), pyrazole (Pyrz, 98 wt%), imidazole (Im, 98 wt%), 1,2,4-triazole (1,2,4-Triz, 98 wt%), 1,2,3-triazole (1,2,3-Triz, 98 wt%), tetrazole (Tetz, 98 wt%) were supplied by Shanghai Aladdin Biochemical Technology Co., Ltd. Tetrabutylammonium hydroxide ([N_{2222}][OH], 25 wt% in H_2O) were obtained from Shanghai Titan Technology Co., Ltd. while ethylene glycol (EG, 99 wt%) was purchased from Shanghai Lingfeng Chemical Reagent Co., Ltd. and succinonitrile (SN, 99 wt%) was supplied by Shanghai Macleane Biochemical Technology Co., Ltd. All regents were used without further purification. The open air which contained about 420–430ppm CO_2 was used after it was dried with CaO. The gas mixtures containing 500 ppm of CO_2 was generated from mixing CO_2 (0.5 vol%) and N_2 (99.99 vol%), while the gas mixtures containing 1 vol %, 2 vol%, 3 vol%, and 4 vol% of CO_2 was generated from mixing CO_2 (5 vol%) and N_2 (99.99 vol%) with the flow rates controlled by mass flow controllers (model: D07-19B, Beijing Sevenstar Electronics Co. Ltd., Beijing, China) with digital read out box (model: D08-3B/ZM, Beijing Sevenstar Electronics Co. Ltd, Beijing, China) and verified by soap bubble flowmeters. CO_2 (0.5 vol%, 5 vol%, and 99.99 vol%) and N_2 (99.99 vol%) were obtained from Hangzhou Jingong Special Gas Co., Ltd. All the CO_2 concentrations (open air, 500 ppm, 0.5 vol%, 1 vol%, 2 vol%, 3 vol%, 4 vol% and 5 vol%) were measured / verified by a non-dispersive infrared CO_2 analyzer (GXH-3010F, Beijing Huayun Analytical Instrument Institution Co., Ltd., China) with the accuracy of 0.001 % (https://www.hyaii.com).

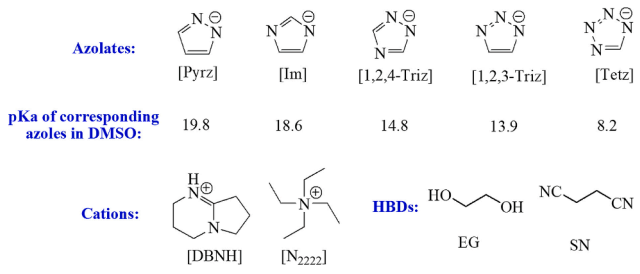

Fig. 1. Structures of anions, cations, and HBDs in this work.

2.2. Synthesis of functional DESs

All kinds of AILs, such as [DBNH][Pyrz], 1,5-diazabicyclo[4.3.0]non-5-enium imidazolate ([DBNH][Im]), 1,5-diazabicyclo[4.3.0]non-5-enium 1,2,4-triazolate ([DBNH][1,2,4,-Triz]), 1,5-diazabicyclo[4.3.0]non-5-enium 1,2,3-triazolate ([DBNH][1,2,3-Triz]), and 1,5-diazabicyclo[4.3.0]non-5-enium tetrazolate ([DBNH][Tetz]), as well as tetraethylamminonium pyrazolate ([N_{2222}][Pyrz]) were prepared by acid-base neutralization of DBN or [N_{2222}][OH] with an appointed proton donor (Pyrz, Im, *etc.*) at 60 °C and atmospheric pressure for 6 h. All functional DESs were prepared through mixing HBAs and HBDs together in certain molar ratios. For example, in a typical synthesis of [DBNH][Pyrz]:EG (1:1), [DBNH][Pyrz] (0.04 mol, 7.69 g) and EG (0.04 mol, 2.48 g) were added together in a round-bottom flask under an atmosphere of N_2. The mixture was stirred at 60 °C for 2 h until turning into a homogeneous and transparent liquid. Then, these DESs dried under vacuum at 60 °C for at least 24 h to remove the reduce the possible trace of water before used.

2.3. Characterization

The chemical structures of these functional DESs before and after the absorption of CO_2 were verified by NMR and FT-IR methods at room temperature, and the instruments were supplied by Bruker (400 MHz NMR and VERTEX 70 IR). Deuterochloroform ($CDCl_3$) and dimethyl sulfoxide-d6 (DMSO-d_6) was used as the solvent and residual $CHCl_3$ (77.16 ppm) and DMSO (39.50 ppm) can be recognized as the internal reference for NMR analyzing. High-resolution mass spectrometry (HR-MS, Thermo Fisher Scientific Q Exactive Focus, Bruker Esquire 3000) equipped with electrosprayionization (ESI) interface and ion-trap analyzer was used to analyze the ionic compounds (ILs and DESs) and obtain the molecular weight (Mw) of ions. The melting points were measured on a NETZSCH DSC 200F3 in the range of −100 to 40 °C at a heating rate of 10 °C min^{-1} under N_2 atmosphere. Using an EG-calibrated pycnometer, densities of DESs were measured in the temperature range of 20–80 °C with an interval of 10 °C under atmospheric pressure. The viscosities of these DESs were determined at the same temperatures using a viscometer supplied from Brookfield (DVNEXT-LV).

2.4. CO_2 capture

The experiments of CO_2 absorption by these functional DESs were carried out according to previous report[43] under atmospheric pressure at various temperatures and different concentration CO_2 in dilute gas streams. In a typical run of CO_2 absorption, gas with different concentration of CO_2 was bubbled into about 1.0 g DES in a glass container with an inner diameter of 10 mm, which was partly immersed in a metal bath of desirable temperature. The flow rate was controlled at about 20 mL min^{-1} using a rotameter (Xinghua Xiangjin Flow Meter Factory, Xinghua, China) with the accuracy of ±6 %, while the standard

uncertainty of absorption temperature $u(T)$ is ±0.1 °C. An electronic balance with the accuracy of ±0.0001 g was used to measure the CO_2 absorption capacities by different DESs at regular intervals. To test the reliability of our absorption equipment and method, [P_{2222}][1,2,4-Triz]: EG (1:2) was prepared and CO_2 capture was measured under the same conditions (25 °C and 1 bar CO_2) as the reference [43]. The results of comparison exhibited no obvious change of capacity between our absorption data and the data in the reference [43], indicating the absorption equipment and method were reliable (Fig. S1). Besides, a process for CO_2 capture from open air (CO_2 concentration: 420–430 ppm) is developed and illustrated in Fig. 2, and the absorption experiments were carried out as similar as CO_2 capture from dilute gas streams. The absorption capacity of CO_2 by DES (Z, in mole of CO_2 per mole of anion) was calculated according to the literatures:

$$Z = \frac{(m_{\text{total}} - m_{\text{DES}})/M_{CO_2}}{m_{\text{DES}}/M_{\text{DES}}} \times \frac{1}{n_{\text{HBA}}}$$

where M_{CO2} and M_{DES} are the molar weights of CO_2 and DES in g mol^{-1}, respectively. M_{DES} could be calculated $M_{\text{DES}} = n_{\text{HBA}} \times M_{\text{HBA}} + n_{\text{HBD}} \times M_{\text{HBD}}$, where M_{HBA} and M_{HBD} are the molar weights of HBA and HBD in g mol^{-1}, and n_{HBA}: n_{HBA} is the molar ratio of HBA: HBD.

3. Results and discussion

3.1. Physical properties

First of all, the molecular ion peak, including cation and anion, of typical ILs [DBNH][Pyrz] and [DBNH][1,2,3-Triz], and corresponding DESs, [DBNH][Pyrz]:EG (1:1) and [DBNH][1,2,3-Triz]:EG (1:1) were determined with HR-ESI-MS under positive ion mode or negative ion mode, and the results were illustrated in Fig. S2. For example, it could be seen that an ion peak at m/z 125.107 in HR-ESIMS spectrum of [DBNH][Pyrz] under positive ion mode could be assigned to [DBNH] cation (Mw of DBN is 124.18 g mol^{-1}) while an ion peak at m/z 67.029 under negative ion mode could be assigned to [Pyrz] anion (Mw of Pyrz 68.08 g mol^{-1}), indicating the formation of [DBNH] cation and [Pyrz] anion *via* acid-base neutralization. Clearly, these peaks both available in the spectra of [DBNH][Pyrz]:EG (1:1) while unavailable in the spectra of DBN-EG (1:1), suggesting the introduction of EG in IL may not affect the structure and ionicity of [DBNH][Pyrz] and the EG (Mw = 62.07 g mol^{-1}) could not be deprotonated in [DBNH][Pyrz]:EG (1:1). Moreover, the melting points of typical ILs and corresponding IL-based DESs were measured, and the results were illustrated in Fig. S3. It is showed that the melting points of [DBNH][Pyrz]:EG (1:1), and [DBNH][1,2,4-Triz]:EG (1:1) are all lower than [DBNH][Pyrz] and [DBNH][1,2,4-Triz], respectively, indicated that these IL-based mixtures were DESs, according to the definition of DESs.

Affected by the structures of DESs and the molar ratios of HBA:HBD, it is clear that density and viscosity are vital rheological properties of a mixture and will affect the CO_2 capture performance.[48–50] Thereby, these properties of [DBNH][Pyrz]:EG 1:1), [DBNH][Im]:EG (1:1), [DBNH][Pyrz]:SN (1:1), and [N_{2222}][Pyrz]:EG (1:1) were measured at different temperatures in the range of 20 °C ~ 80 °C under atmospheric pressure, and the values are listed in Table S1. It can be seen that the density (ρ, in g cm^{-3}) and viscosity (η, in mPa·s) are inversely proportional to temperature. With the temperature increase, both the denticity and the viscosity decreased, and vice versa, due to the increase in volume. The values of density were around 1 g cm^{-3} while that of the viscosity were in a large range of 159.4–1.48 mPa·s. Clearly, the lowest density and the largest viscosity could be found in [N_{2222}][Pyrz]:EG (1:1) at any temperature, indicating these properties are greatly influenced by the structures of DESs. The relations between density and temperature and between viscosity and temperature could be described by the following linear equations, respectively.

$$\ln\rho = a + b\,T$$

and

$$\ln\eta = \ln\eta_0 + \frac{E_\eta}{RT}$$

where a and b are fitting constants, η_0 denotes the pre-exponential constant in mPa·s, E_η represents the flow activation energy in kJ mol^{-1}, T is the experimental temperature in K, and R is the universal gas

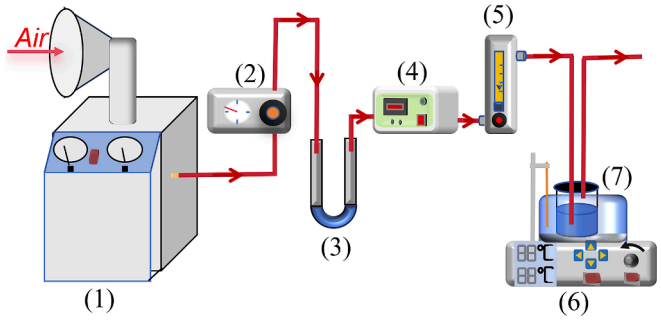

Fig. 2. Apparatus of CO_2 capture from open air: (1) Air generator containing CO_2 ; (2) high pressure valve; (3) drying tube with anhydrous $CaCl_2$; (4) CO_2 analyzer; (5) rotameter; (6) magnetic stirrer with thermocouple; (7) glass bottle filled with DES.

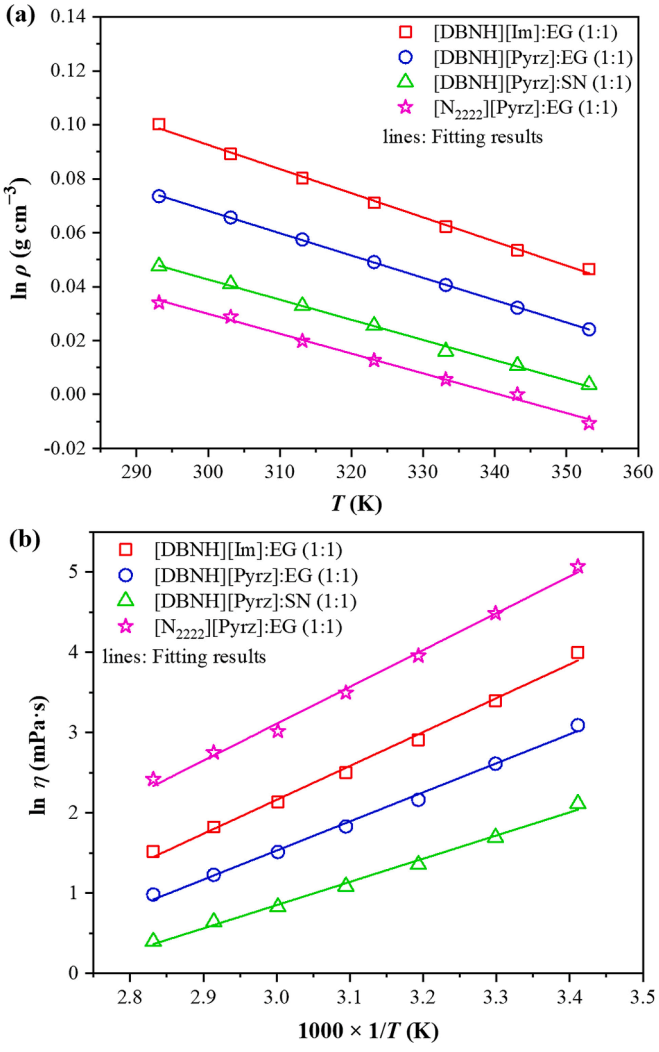

Fig. 3. Linear relationship for density (a) and viscosity (b) with the temperature.

constant (8.314 J K^{-1} mol^{-1}). The fitting curves were illustrated in Fig. 3 and the parameters were listed in Table S2. The fitting results showed that the values of E_η decreased in the order: [N_{2222}][Pyrz]:EG (1:1) > [DBNH][Im]:EG (1:1) > [DBNH][Pyrz]:EG (1:1) > [DBNH][Pyrz]:SN (1:1). Coefficient of thermal expansion of DESs (α_p, in K^{-1}) is the rate at which the volume of a DES (V, in cm^3 mol^{-1}) changes with respect to the temperature (T, in K) change, as the following equation:

$$\alpha_p = \frac{1}{V} \times \left(\frac{\partial V}{\partial T}\right)_p = -\left(\frac{\partial \ln \rho}{\partial T}\right)_p$$

The values of α_p were listed in Table S3. Clearly, the values of α_p decreased in the order: [DBNH][Im]:EG (1:1) > [DBNH][Pyrz]:EG (1:1) > [DBNH][Pyrz]:SN (1:1) > [N_{2222}][Pyrz]:EG (1:1). The higher thermal coefficient value indicates higher free volume of fluids.

3.2. CO_2 capture

3.2.1. Effects of structures of DESs

A DES includes three parts, cation, anion, and HBD. Thus, the structures of cation, anion and HBD inevitably affect the performance of CO_2 capture by DESs. As the anion plays a key role in CO_2 capture by ILs, the effect of anion with different structures was first investigated and the results were illustrated in Fig. 4. It can be seen that the CO_2 capture capacities of [DBNH][Pyrz]:EG (1:1), [DBNH][Im]:EG (1:1), [DBNH][1,2,4-Triz]:EG (1:1), [DBNH][1,2,3-Triz]:EG (1:1), and [DBNH][Tetz]:EG (1:1) were 26 wt% (5.91 mmol g^{-1}), 19 wt% (4.32 mmol g^{-1}), 13 wt% (2.95 mmol g^{-1}), 10 wt% (2.27 mmol g^{-1}), and 2 wt% (0.45 mmol g^{-1}) at 20 °C under 5 vol% CO_2, respectively. It is known that the structure of azoles, including the position and the amount of N atoms, affect the basicity of azolate anions. Thus, the relationship between pKa of azoles and the CO_2 capture capacities of these azolate-based DESs was further studied, and the result was revealed in Fig. 5 and Table S4. With the increase of pKa of azoles, the CO_2 capacity of these azolate-based DESs increased linearly with R^2 = 0.96. That is, [DBNH][Pyrz]:EG (1:1) obtained the highest CO_2 capacity because of the pyrazole with the highest pKa value (19.8 in DMSO). Besides, it is safely predicted that anions with pKa < 7.9 in DMSO would not absorb CO_2 at all. This value near the pKa of carbonic acid (pKa = 6.36 in H_2O and aqueous pKa < DMSO pKa by 1 ~ 13 units).[51] There by, pyrazolate anion was selected for the following investigations.

The molar ratio of HBA:HBD is not only affects the density and viscosity of DES, but also affects the CO_2 absorption capacity. Thus, the performances of CO_2 capture by [DBNH][Pyrz]:EG (2:1), [DBNH][Pyrz]:EG (1:1), and [DBNH][Pyrz]:EG (1:2) were investigated, and the results were illustrated in Fig. 6. It can be seen that the capacities of these DESs were 20 wt% (4.55 mmol g^{-1}), 26 wt% (5.91 mmol g^{-1}), and 16 wt% (3.64 mmol g^{-1}) at 20 °C under 5 vol% CO_2, respectively. The results indicated that the concentration of IL cannot be too high or too low, possibly because of the reaction mechanism. In addition, CO_2 capacity of [DBNH][Pyrz]:SN (1:1) was only 17 wt% (3.86 mmol g^{-1}) at 20 °C under 5 vol% CO_2, indicating the hydroxyl groups in the EG is also the active sites for CO_2 capture by AIL-based DESs. Moreover, an aprotic cation tetrabutylammonium ([N_{2222}]) was selected to test the effect of the structure of cation in DES on CO_2 capture. The results also could be found in Fig. 6. CO_2 capacity of [N_{2222}][Pyrz]:EG (1:1) was also 16 wt% at 20 °C under 5 vol% CO_2, indicating the proton on the cation is beneficial for CO_2 absorption.

Moreover, the viscosities of [DBNH][Pyrz]:EG (2:1), [DBNH][Pyrz]:EG (1:1), [DBNH][Pyrz]:EG (1:2) and [DBNH][Pyrz]:SN (1:1) DESs and their correspondent neat IL [DBNH][Pyrz] before and after CO_2 saturation at 20 °C under 5 vol% CO_2 were also measured to investigate the effect of EG and SN, the results were illustrated in Table 1. It can be seen

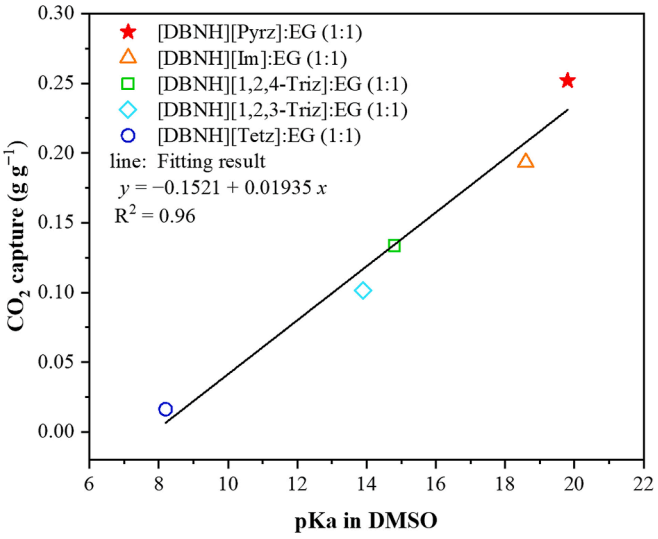

Fig. 5. Relationship between pKa of azoles and the CO_2 capture capacities of DESs.

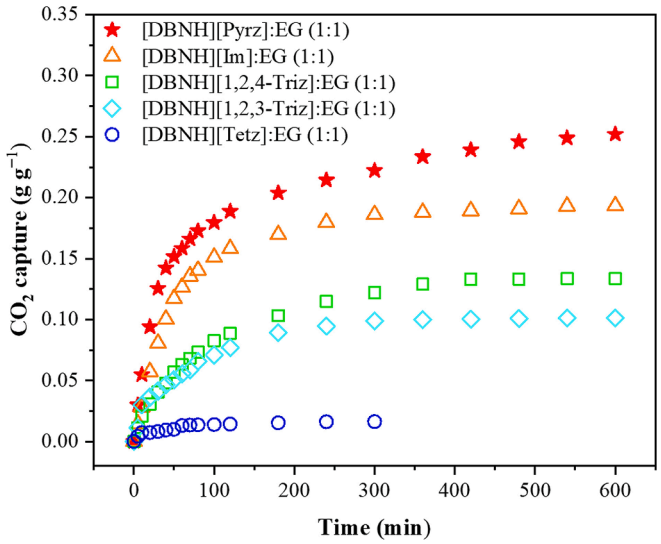

Fig. 4. Effect of structures of azolate anion on the CO_2 absorption by DESs at 20 °C under 5 vol% CO_2 .

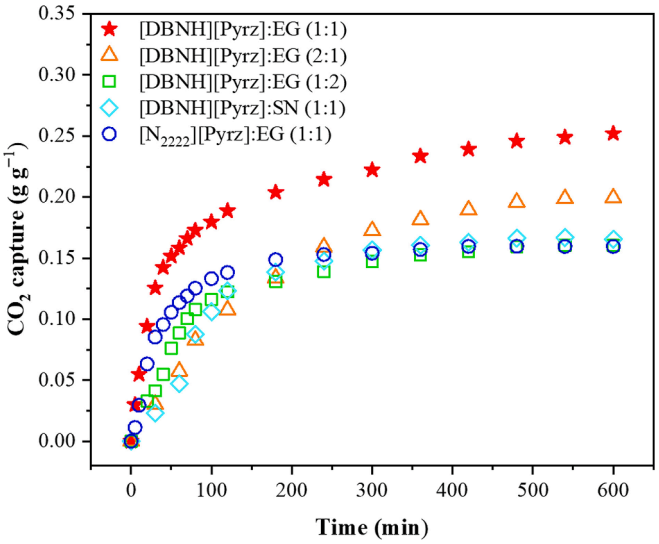

Fig. 6. Effect of molar ratio of HBA:HBD and the structures of cations and HBAs on the performance of CO_2 absorption by DESs at 20 °C under 5 vol% CO_2 .

Table 1
Comparison of viscosity of DESs and neat IL before and after CO_2 saturation at 20 °C under 5 vol% CO_2 .

Absorbent [a]	Viscosity (mPa s)		Viscosity Increase (fold) [b]	CO_2 Capacity		
	Before CO_2 capture	After CO_2 capture		mmol/g	g/g	mol/mol [c]
[DBNH][Pyrz]:EG (2:1)	26.56	407.7	15.35	4.55	0.20	1.02
[DBNH][Pyrz]:EG (1:1)	22.03	263.2	11.95	5.91	0.26	1.50
[DBNH][Pyrz]:EG (1:2)	28.05	116.5	4.15	3.64	0.16	1.31
[DBNH][Pyrz]:SN (1:1)	8.28	88.6	10.7	3.86	0.17	1.05
[DBNH][Pyrz]	12.23	1032	84.38	2.63	0.16	0.70

[a] Molar ratio in brackets.
[b] Viscosity of the absorbents saturated with CO_2 relative to CO_2-free absorbents.
[c] CO_2 capacity in mol/mol, meaning mole of CO_2 per mole of [Pyrz] anion.

that the increased viscosity could be obtained for [DBNH][Pyrz]:EG DESs while the decreased viscosity could be obtained for [DBNH][Pyrz]:SN, due to the strong hydrogen bonding of formers. After CO_2 saturation, the viscosity of all absorbents increased, and the increased folds for ILs are more than DESs, due to the strong interaction between cation and anion in formers. Besides, CO_2 capacity of neat IL [DBNH][Pyrz] was only 6 wt% (3.86 mmol g^{-1}) while that of [DBNH][Pyrz]-based DESs was more than 15 wt% (3.42 mmol g^{-1}). While for CO_2 capture in the unit of mol/mol (mole of CO_2 per mole of [Pyrz] anion), the results indicated that suitable HBD (EG with molar ratio of [DBNH][Pyrz]:EG = 1:1) could promote the absorption of CO_2. Fig. 7 illustrated the CO_2 absorption by three kinds of absorbents, a switchable solvent DBN-EG (1:1), an IL [DBNH][Pyrz], and a DES [DBNH][Pyrz]:EG (1:1). It can be seen that CO_2 capacity of [DBNH][Pyrz]:EG (1:1) is 26 wt% (5.91 mmol g^{-1}) while that of DBN-EG (1:1) is 0.21 wt% (4.77 mmol g^{-1}), indicating that the introduction of Pyrz and formation of [Pyrz] could actually increase the CO_2 absorption capacity per unit mass (g/g) of the absorbent. Additionally, the absorption capacity per unit molar (mol/mol) reflecting the reactivity of solvents, and the CO_2 capacities of [DBNH][Pyrz]:EG (1:1) and DBN-EG (1:1) were 1.50 and 0.91 mol of CO_2 per mole of solvent, also indicating the introduction of Pyrz and formation of [Pyrz] anion is efficient for CO_2 capture. Thus, suitable EG and formation of [Pyrz] in [DBNH][Pyrz]:EG (1:1) system are both play a key role in CO_2 capture. Based on the comprehensive considerations, [DBNH][Pyrz]:EG (1:1) DES was selected for future investigations.

3.2.2. *Effects of CO_2 partial pressure and temperature*

The performances of CO_2 capture by [DBNH][Pyrz]:EG (1:1) under different CO_2 partial pressures, particularly in the range of 500 ppm ~ 5 vol% CO_2 (CO_2 partial pressure 0.0005–0.05 bar), were studied. It is shown in Fig. 8 that the saturated CO_2 capture capacity at 20 °C and 0.05 bar was 26 wt% CO_2. As the CO_2 partial pressure decreased to 0.01 bar, the CO_2 absorption capacity of 23 wt% (5.23 mmol g^{-1}) could still be reached, indicating the efficient CO_2 absorption of these DESs. To the best of our knowledge, these are the highest capacities for CO_2 absorption by DESs and ILs under low concentrations of CO_2 (Table 2). Recently, it is reported that the concentration of CO_2 reached 413.2 ± 0.2 ppm by 2021 [52] and will increase to 500 ppm by 2050. [53] Thus, 500 ppm CO_2 was used to test whether the [DBNH][Pyrz]:EG (1:1) DES is suitable for the direct capture of CO_2 from ambient air, or "direct air capture" (DAC) [54–56] The results showed that as high as 14 wt% (3.18 mmol g^{-1}) CO_2 could be captured at 20 °C and 0.0005 bar CO_2, indicating the [DBNH][Pyrz]:EG (1:1) DES could be used as an alternative sorbent for DAC application. Moreover, the effect of absorption temperature on the CO_2 absorption by [DBNH][Pyrz]:EG (1:1) was investigated and the results were also illustrated in Fig. 8. CO_2 absorption capacity was found to be decreased with the increase of absorption temperature. For example, when the absorption temperature increased from 20 °C to 60 °C, the CO_2 absorption capacity decreased from 26 wt% to 10 wt% (2.27 mmol g^{-1}) under 0.05 bar CO_2. Additionally, CO_2 capture from open air with the CO_2 concentration between 420 to 430 ppm has been investigated, and the results were listed in Table 3. It can be seen that higher CO_2 capacities could be obtained by [DBNH][Pyrz]:EG (1:1), [N_{2222}][Pyrz]:EG (1:1), and [DBNH][Im]:EG (1:1), while lower capacities were obtained by [DBNH][1,2,3-Triz]:EG (1:1) and [DBNH][1,2,4-Triz]:EG (1:1), probably due to the high basicity of Pyrz and Im but low basicity of 1,2,3-Triz and 1,2,4-Triz, which consisted with the relationship between pKa of azoles and the CO_2 capture capacities of DESs.

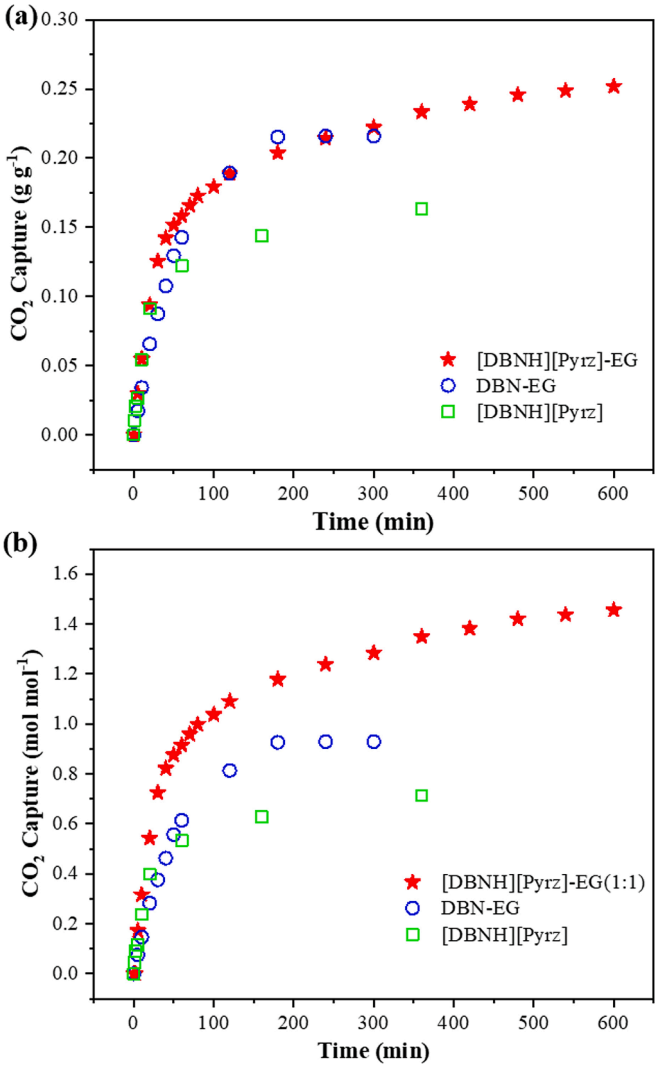

Fig. 7. CO_2 absorption by [DBNH][Pyrz]:EG (1:1), DBN-EG (1:1), and [DBNH][Pyrz] at 20 °C under 5 vol% CO_2 .

Above results indicated that the absorbed CO_2 could be released and the DES could be recycled *via* either heating or bubbling N_2 through the CO_2-saturated DES. Thus, the desorption of captured CO_2 from CO_2-saturated [DBNH][Pyrz]:EG (1:1) and the recycle of [DBNH][Pyrz]:EG (1:1) have been investigated (Fig. 9). It can be seen from Fig. 9a that CO_2

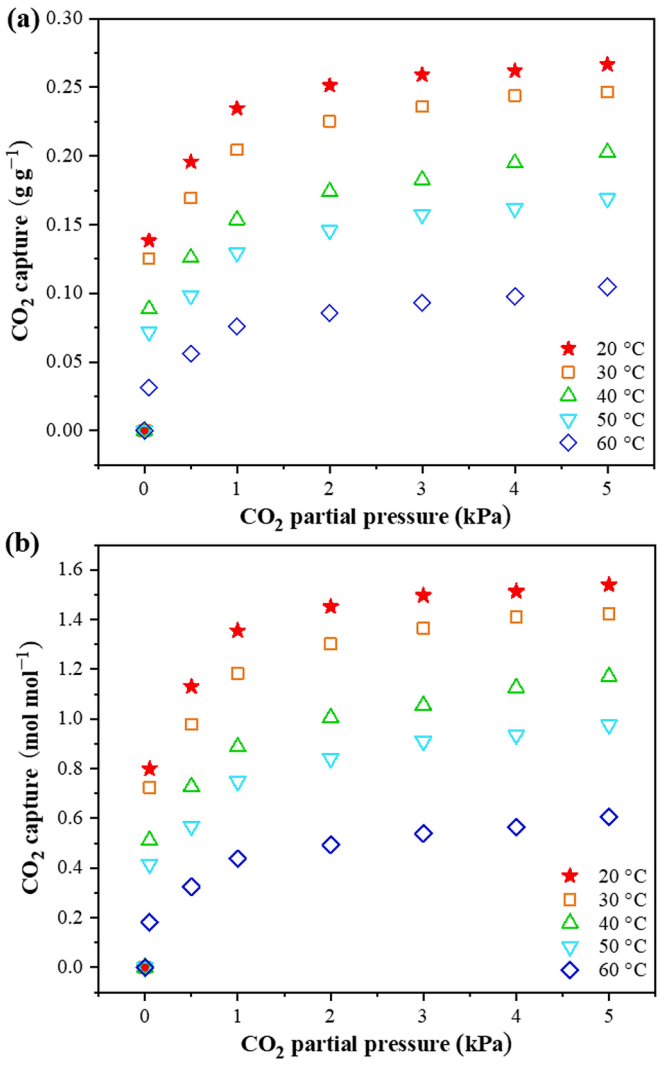

Fig. 8. CO_2 capture by [DBNH][Pyrz]:EG (1:1) under different CO_2 partial pressures and absorption temperatures.

could be desorbed at 60 °C under N_2, which is milder than the desorption conditions reported in most previous work. The [DBNH][Pyrz]:EG (1:1) DES could be recycled seven times and the CO_2 capacity could be maintained (Fig. 9b).

3.2.3. *Possible mechanism of CO_2 absorption*

The mechanism of CO_2 absorption by [DBNH][Pyrz]:EG (1:1) was systematically studied. Fig. 10 shows the change of ^{13}C NMR spectroscopy of [DBNH][Pyrz]:EG (1:1) before and during the CO_2 absorption at 20 °C under 0.05 bar. Compared with the ^{13}C NMR spectrum of fresh [DBNH][Pyrz]:EG (1:1), when 5 wt% (1.14 mmol g^{-1}) CO_2 was captured, a strong signal at 158.4 ppm and a weak signal at 158.0 ppm were produced. Interestingly, these signals were moved first down-field when 10 wt% CO_2 was captured and then up-field to 158.3 and 157.8 ppm when 15 wt% CO_2 was captured, indicating a change in the chemical environment surrounding these carbon atoms. It is clear that another new signal at 160.5 ppm was produced when 15 wt% CO_2 was captured. The intensity of the former two signals were slightly decreased while the latter one signal was slightly increased during more CO_2 absorbed in [DBNH][Pyrz]:EG (1:1). At last, the former signals appeared at 158.8 and 158.4 ppm while the latter signal appeared at 161.0 ppm in the ^{13}C NMR spectrum of CO_2-saturated [DBNH][Pyrz]:EG (1:1). Based on the previous reports,[43,62,68,72] all these three signals would be attributed to carbonyl carbons of O···CO_2 carbonate species and/or

Table 2
Comparison of CO_2 capacities of [DBNH][Pyrz]:EG (1:1) with other DESs and ILs.

Absorbent[a]	*T* (°C)	*P* (bar)	CO_2 Capacity		Ref.
			(mmol/g)	(g/g)	
[DBNH][Pyrz]:EG (1:1)	40	0.05	4.55	0.20	This work
[DBNH][Pyrz]:EG (1:1)	30	0.05	5.68	0.25	This work
[DBNH][Pyrz]:EG (1:1)	20	0.05	5.91	0.26	This work
[DBNH][Pyrz]:EG (1:1)	20	0.02	5.68	0.25	This work
[DBNH][Pyrz]:EG (1:1)	20	0.01	5.23	0.23	This work
[DBNH][Pyrz]:EG (1:1)	20	0.0005	3.18	0.14	This work
[DBNH][Pyrz]:EG (1:1)	20	open air	3.18	0.14	This work
DBN:[Bmim][Cl]:Im (1:1:2)	25	1	2.46	0.1082	[57]
DBN:[Bmim][Cl]:Im (1:2:1)	25	1	1.79	0.0788	[57]
DBN:[Bmim][Cl]:Im (1:1:1)	25	1	2.78	0.1223	[57]
[Bmim][Cl]:MEA (1:1)	25	1	1.91	0.084	[37]
[DEAH][Cl]:MDEA (1:3)	25	1	2.46	0.1082	[58]
[MEAH][Cl]:MEA (1:4)	20	1	5.68	0.25	[59]
[Ch][Cl]:MEA (1:5)	30	1	5.73	0.2523	[60]
[MDEAH][Cl]:MDEA (1:3)	25	1	1.35	0.0594	[58]
$[N_{2222}]$[Thy]:EG (1:2)	25	1	2.23	0.0981	[61]
$[N_{2222}]$[Car]:EG (1:2)	25	1	2.15	0.0948	[61]
[DBUH][Car]:EG (1:2)	25	1	2.27	0.1000	[62]
[DBUH][Thy]:EG (1:2)	25	1	2.27	0.1000	[62]
[TETAH][Cl]:thymol (1:3)	40	1	2.05	0.09	[38]
[TETAH][Cl]:thymol (1:3)	40	0.1	0.93	0.0411	[38]
$[TEPAH_2][Im]_2$:EG (1:4)	25	1	3.95	0.1736	[63]
$[DETAH_2][Im]_2$:EG (1:2)	25	1	5.08	0.2235	[63]
$[P_{2222}]$[Triz]:EG (1:2)	25	1	2.68	0.118	[43]
$[N_{2222}]$[Triz]:EG (1:2)	25	1	2.84	0.125	[43]
[Emim][2-CNpyr]:EG (1:2)	25	1	2.59	0.114	[64]
[Emim][Gly] + [Emim][Ac] (1:1)	25	1	2.95	0.13	[65]
[Emim][Gly] + [Emim][Ac] (1:1)	25	0.15	2.05	0.09	[65]
[DMAPAH][Ac] + EDA[b]	30	1	5.91	0.260	[66]
[DMAPAH][Ac] + EDA[b]	30	0.1	4.70	0.207	[66]
[MTBDH][Im]	23	1	4.65	0.20	[67]
$[P_{66614}]$[Pyrz]	23	1	1.85	0.08	[40]
$[P_{66614}]$[2-PyO]	20	1	2.73	0.12	[68]
$[P_{4442}]_2$[IDA]	40	1	2.85	0.13	[25]
$[P_{4442}]$[Suc]	20	1	5.68	0.25	[69]
$[P_{4442}]$[Suc]	20	0.1	5.01	0.22	[69]
$[N_{1111}]$[Eaca]	40	1	4.09	0.18	[70]
$[N_{1111}]$[Eaca]	40	0.1	2.95	0.13	[70]
[Cho][Triz]	40	1	3.41	0.15	[71]
$[P_{4446}]$[Im]	30	0.0004	1.92	0.08	[23]
$[P_{4446}]$[BenIm]	30	0.0004	1.31	0.06	[23]

[a] molar ratio in brackets.
[b] mass ratio 1:1.

N···CO_2 carbamate species. Firstly, the signal at 158.4 ppm can be assigned to the carbonyl carbon of O···CO_2 in [EG − CO_2] anion formed between the reaction of [EG] anion and CO_2, and the [EG] anion was produced through deprotonation of EG by [Pyrz]. The signals of EG, [EG], and [EG − CO_2] were in the range of 60 ~ 67 ppm. It can be seen that 63.0 ppm for the carbon of two same methylene groups in EG in the spectrum of fresh DES has been shifted to 62.8 ppm as well as two other new signals at 66.3 and 60.7 ppm were appeared after the absorption of 5 wt% CO_2, attributing to two different carbons of methylene groups in unsymmetrical carbonate [EG − CO_2] anion. Secondly, it is interesting that the signal at 158.0 ppm, accompanied by the signal at 158.4 ppm, in the ^{13}C NMR spectrum of DES + CO_2 (5 wt%), might be expected the

Table 3
CO_2 capture from open air (CO_2 concentration between 420 to 430 ppm) at 20 °C.

Absorbent[a]	Time (h)	CO_2 Capacity		
		mmol/g	g/g	mol/mol [c]
[DBNH][Pyrz]:EG (1:1)	48	3.18	0.14	0.81
$[N_{2222}]$[Pyrz]:EG (1:1)	24	2.73	0.12	0.71
[DBNH][Im]:EG (1:1)	48	2.05	0.09	0.52
[DBNH][1,2,3-Triz]:EG (1:1)	24	1.14	0.05	0.29
[DBNH][1,2,4-Triz]:EG (1:1)	24	0.91	0.04	0.23

[a] Molar ratio in brackets.
[c] CO_2 capacity in mol/mol, meaning mole of CO_2 per mole of anion.

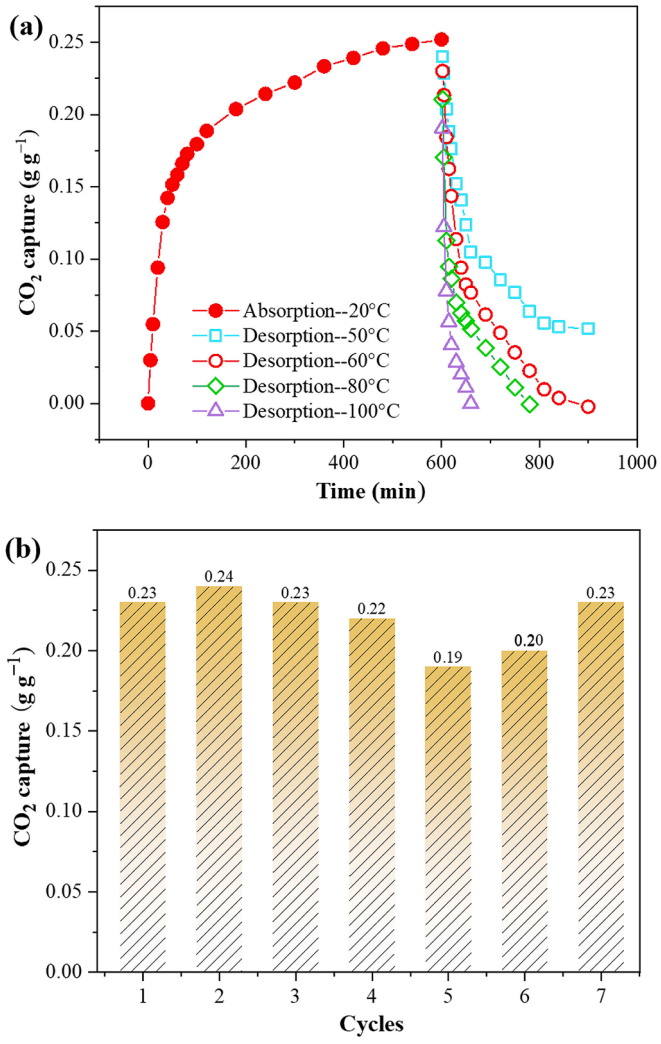

Fig. 9. (a) The desorption of captured CO_2 from CO_2 -saturated [DBNH][Pyrz]:EG (1:1) and (b) the recycle of [DBNH][Pyrz]:EG (1:1).

formation of symmetrical biscarbonate $[CO_2 - EG - CO_2]^{2-}$ anion.[73] Another evidence for $[CO_2 - EG - CO_2]^{2-}$ anion formation was that a new signal at 63.6 ppm appeared in the spectrum of [DBNH][Pyrz]:EG (1:1) after the absorption of 5 wt% CO_2, different from the signal at 63.0 ppm in the spectrum of fresh [DBNH][Pyrz]:EG (1:1). It can be seen that the intensity of both shifts at 158.0 and 63.6 ppm first increased and then decreased simultaneously during the absorption of more CO_2. Thirdly, the signal at 160.5 ppm appeared in the spectrum of DES after the absorption of 15 wt% CO_2 can be assigned to the carbonyl carbon of N···CO_2 in [Pyrz – CO_2] anion formed *via* the reaction between [Pyrz] anion and CO_2, according to the previous reports.[40,69] Additionally, an interesting result is that the amount of $[CO_2 - EG - CO_2]^{2-}$ and [EG – CO_2] species decreased while [Pyrz – CO_2] species increased during more than 15 wt% CO_2 was captured. Moreover, in the ^{13}C NMR spectrum of fresh [DBNH][Pyrz]:EG (1:1), a typical signal at 161.2 ppm, assigning to the carbon of –N–C – N – in [DBNH] cation, was obviously shifted down-field to 163.8 ppm during CO_2 absorption, because of the interaction between [DBNH] cation and carboxylate anions.[74].

Furthermore, the comparison of ^{13}C NMR spectra of [DBNH][Pyrz]:SN (1:1) and $[N_{2222}]$[Pyrz]:EG (1:1) with [DBNH][Pyrz]:EG (1:1) before and after CO_2 absorption at 20 °C under CO_2 partial pressure of 0.05 bar were used to further verify the different carbonyl carbons of and O···CO_2 carbonate species and N···CO_2 carbamate species (Fig. 11). It can be seen that compared with two new shifts at 160.9 and 158.4 ppm were present in the ^{13}C NMR spectrum of [DBNH][Pyrz]:EG (1:1) + CO_2, only one new shift at 160.7 ppm was present in the ^{13}C NMR spectrum of [DBNH][Pyrz]:SN (1:1) + CO_2, while two new shifts at 160.4 and 157.8 ppm were present in the ^{13}C NMR spectrum of $[N_{2222}]$[Pyrz]:EG (1:1) + CO_2. These results clearly showed that that 163 ppm as well as 159.5 ppm were both appeared while 157.5 and 157.3 ppm were both absent.

Moreover, the mechanism of CO_2 absorption by [DBNH][Pyrz]:EG (1:1) was further investigated by FT-IR spectroscopy (Fig. 12). It can be seen that the intensity of three new stretching vibration peaks at 1682, 1625 and 1310 cm^{-1} increased gradually during CO_2 absorption. These peaks could be assigned to a stretching C═O vibration in N–CO_2 (ν = 1682 cm^{-1}), two stretching C═O vibrations in O–CO_2 (ν = 1625 cm^{-1}), and one stretching C–O vibration (ν = 1310 cm^{-1}) according to the previous reports.[69,75] Although it is impossible to distinguish different C═O vibrations in [EG–CO_2] and $[CO_2$–EG–$CO_2]^{2-}$, it is clear that the cooperative interaction were formed during more CO_2 absorption. Besides, other three new peaks at 3139, 2975 and 2886 cm^{-1} increased gradually during CO_2 capture. Based on the previous reports,[76,77] the first peak could be attributed to N–H stretching vibration in neutral molecule Pyrz, while other two peaks belong to COO···H hydrogen bonds. Due to the deprotonation of –OH in EG by [Pyrz] anion, the peak at 960 cm^{-1} belong to the bending vibration of –OH decreased gradually during CO_2 capture.[78] Thus, these results suggested that the anion-induced multi-site cooperations of O···CO_2 and N···CO_2 were the main reason of ultrahigh CO_2 capacities.

Based on the observed products and previous reports,[79–81] the possible mechanism of CO_2 capture by [DBNH][Pyrz]:EG (1:1) could be proposed as Fig. 13. It showed that these reactions were initiated by [Pyrz] anions and resulted in two routes with three forms of absorbed CO_2, including two kinds of O···CO_2 carbonates and a kind of N···CO_2 carbamate.

3.2.4. *Thermodynamics analysis of CO_2 absorption*

It is clear that the multi-site cooperations of CO_2 capture by [DBNH][Pyrz]:EG (1:1) simultaneously included several reactions and resulted in the difficulty in the analysis of thermodynamic properties, such as the chemical equilibrium constant (K), the change of molar enthalpy of the reaction ($\Delta_r H_m$), the change of molar entropy of the reaction ($\Delta_r S_m$), and the change of molar Gibbs free energy of the reaction ($\Delta_r G_m$), for each reaction. However, it is probably to estimate these properties as the apparent chemical equilibrium constant (K', in dimensionless), the apparent change of molar enthalpy of the reaction ($\Delta_r H'_m$, in kJ mol^{-1}), the apparent change of molar entropy of the reaction ($\Delta_r S'_m$, in J mol^{-1} K^{-1}), and the apparent change of molar Gibbs free energy of the reaction ($\Delta_r G'_m$, in kJ mol^{-1}).[82,83] That is because of all cooperative reactions were induced by [Pyrz] anion through 1:1 equimolar chemical reaction and can be considered as [Pyrz] + CO_2 → [Pyrz]·CO_2 under low concentration CO_2 (particularly 500 ppm).

Here, the apparent thermodynamics analysis of CO_2 absorption by [DBNH][Pyrz]:EG (1:1) was investigated *via* testing the CO_2 absorption capacities at different temperatures (20, 30, 40, 50, and 60 °C) in the units of wt% and mole of CO_2 per mole of [Pyrz] under CO_2 partial pressure of 0.0005 bar. The K' could be obtained by the following

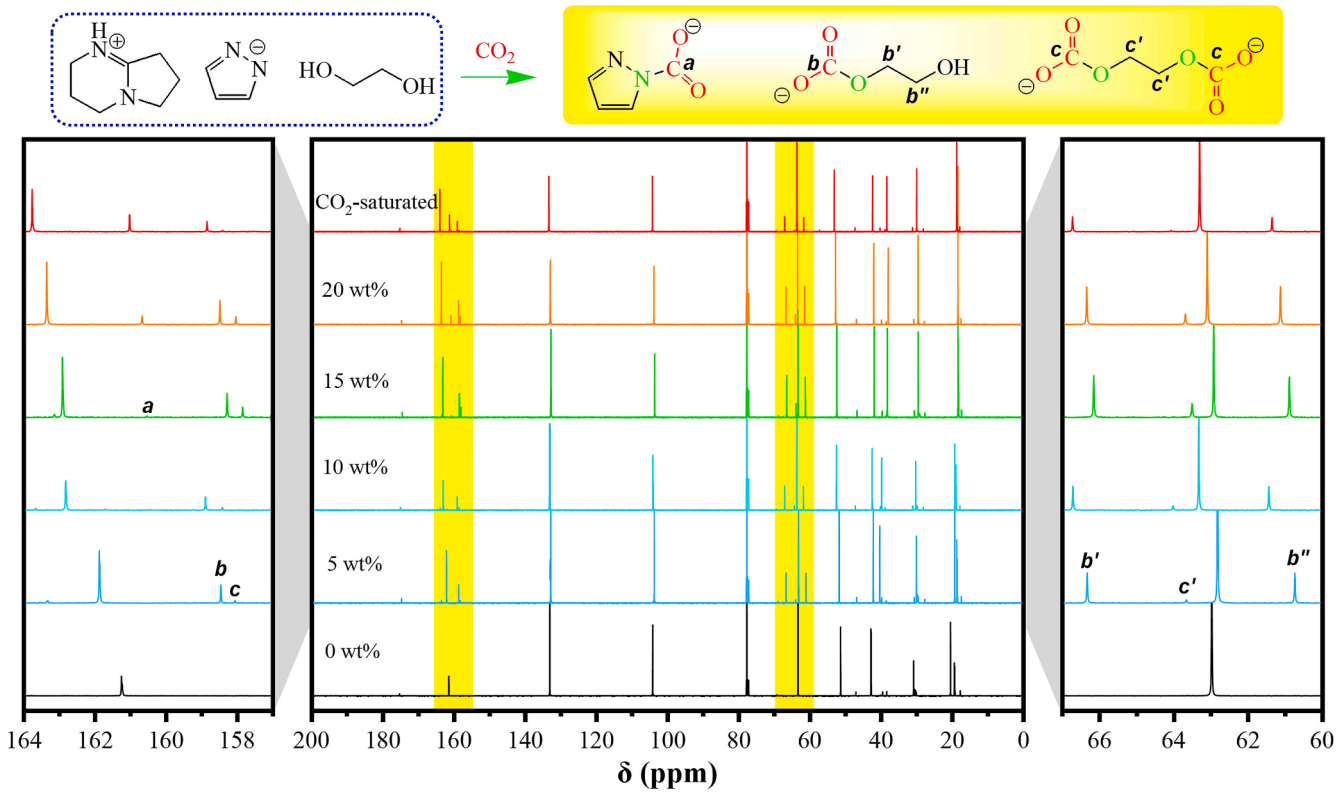

Fig. 10. Comparison of ^{13}C NMR spectra of [DBNH][Pyrz]:EG (1:1) before and during CO_2 absorption at 20 °C under CO_2 partial pressure of 0.05 bar (solvent: $CDCl_3$).

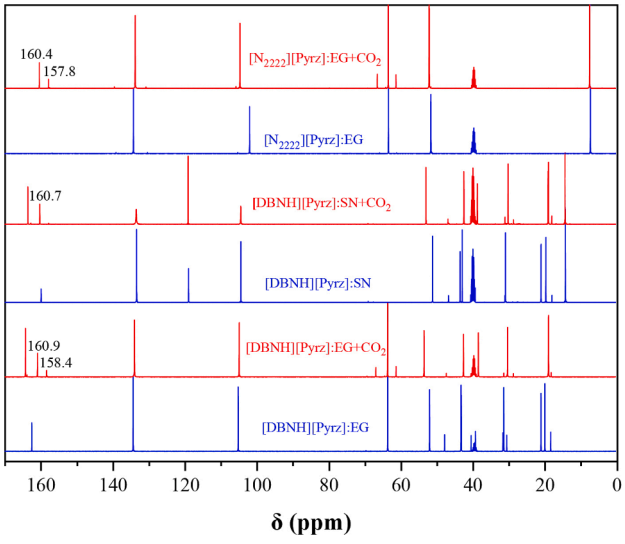

Fig. 11. Comparison of ^{13} C NMR spectra of [DBNH][Pyrz]:EG (1:1), [DBNH][Pyrz]:SN (1:1), and [N_{2222}][Pyrz]:EG (1:1) before and after CO_2 absorption at 20 °C under CO_2 partial pressure of 0.05 bar (solvent: d6-DMSO).

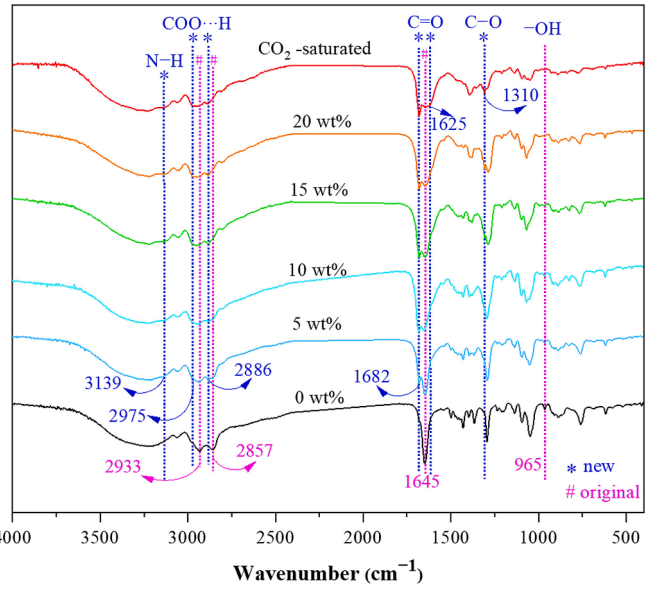

Fig. 12. Comparison of FT-IR spectra of [DBNH][Pyrz]:EG (1:1) before and after the absorption of CO_2 at 20 °C and 0.05 bar.

equation:

$$K' = \frac{Z_{chem}}{(1 - Z_{chem})P/P^{\theta}}$$

where Z_{chem} is the chemical absorption capacity in mole of CO_2 per mole of [Pyrz]. The capacity at different temperatures in different units as well as the calculated values of K' and lnK' were listed in Table 4. K' and lnK' values decreased with the increase of temperature. For the instance, K' at 20, 30, 40, 50, and 60 °C were 7955, 5220, 2092, 1422, and 443.5, respectively, suggesting that CO_2 absorption could be easily performed at low temperature. Due to the quite narrow temperature range, the thermodynamic properties of $\Delta_r H'_m$, $\Delta_r S'_m$, and $\Delta_r G'_m$ could be readily obtained by the following equations from lnK', T (in K), and ideal gas constant R (8.314 J·mol^{-1} K^{-1}):

$$\ln K' = -\frac{\Delta_r H'_m}{RT} + \frac{\Delta_r S'_m}{R}$$

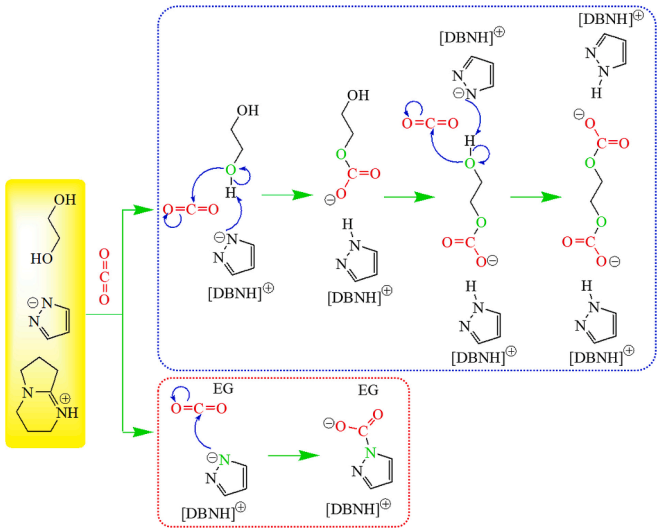

Fig. 13. Plausible reaction mechanism of CO_2 capture by [DBNH][Pyrz]:EG (1:1). Note that all hydrogen bonds are not illustrated.

Table 4
Absorption capacities and thermodynamic properties for the CO_2 capture by [DBNH][Pyrz]:EG (1:1) at different temperatures under CO_2 partial pressure of 0.0005 bar.

T (°C)	CO_2 capture capacity		Parameter		
	g/g	mol CO_2 mol^{-1} [Pyrz]	$1/T$ (in 1/K)	K'	lnK'
20	0.14	0.80	3.411	7955	8.982
30	0.13	0.72	3.298	5220	8.560
40	0.09	0.51	3.193	2092	7.646
50	0.07	0.42	3.094	1422	7.260
60	0.03	0.18	3.001	443.5	6.095

$$\Delta_r G'_m = \Delta_r H'_m - T\Delta_r S'_m$$

The relationship between lnK' and $1/T$ was illustrated in Fig. 14, while Table 5 listed the calculated values of $\Delta_r H'_m$, $\Delta_r S'_m$, and $\Delta_r G'_m$. The results showed that the values of $\Delta_r H'_m$ and $\Delta_r G'_m$ were negative, indicating a spontaneous and exothermic process of CO_2 absorption by DES. Besides, the value of $|\Delta_r H'_m|$ was higher than 50 kJ mol^{-1}, indicating that the interactions between DES and CO_2 were chemically.

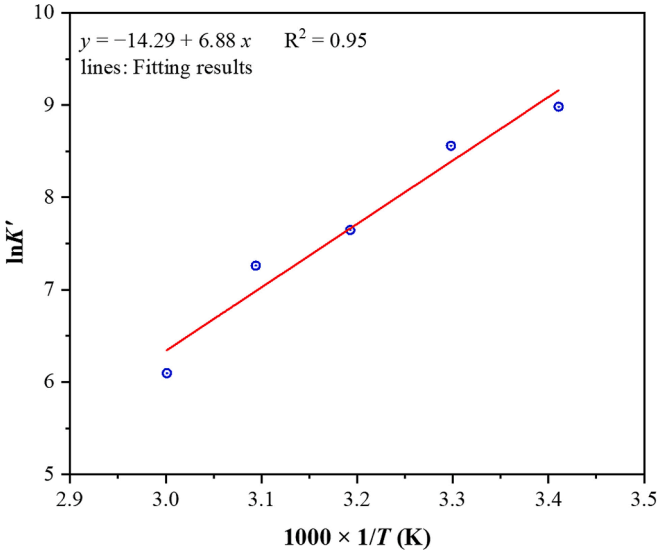

Fig. 14. Slope of the linear relationship between lnK' and $1/T$.

Table 5
Thermodynamic properties for the CO_2 capture by [DBNH][Pyrz]:EG (1:1) at different temperatures under CO_2 partial pressure of 0.0005 bar.

Thermodynamic property	T (°C)				
	20	30	40	50	60
$\Delta_r H'_m$ (kJ mol^{-1})	−57.16				
$10^3\Delta_r S'_m$ (kJ mol^{-1} K^{-1})	−118.8				
$\Delta_r G'_m$ (kJ mol^{-1})	−22.33	−21.14	−19.95	−18.76	−17.58

Additionally, the value of $\Delta_r S'_m$ was also negative, suggesting that the disorder degree became smaller after CO_2 absorption, another result of strong chemical interaction. Generally, because of $\Delta_r H'_m < 0$ and $\Delta_r S'_m < 0$ as well as $|\Delta_r H'_m| > |T\Delta_r S'_m|$, the sign of the value of $\Delta_r G'_m$ was determined by that of $\Delta_r H'_m$. Therefore, $\Delta_r H'_m$ is more favorable than other thermodynamic properties for CO_2 capture under low concentration CO_2 through chemical absorption.

4. Conclusions

In summary, a series of functional DESs forming from azolate ionic liquids as HBAs and EG or SN as HBDs were developed for CO_2 capture. Density and viscosity as well as flow activation energies of these functional DESs were calculated. The performances of CO_2 capture were tested under different temperatures and CO_2 partial pressures (500 ppm–5 vol%). The results showed that, compared with different structures of these azolate-based DESs, the CO_2 capacity increased linearly with the increase of pKa of azoles, and the highest CO_2 capacity could be achieved by [DBNH][Pyrz]:EG (1:1). Compared with other DESs and ILs, the extremely high CO_2 capture capacities of 14 wt% (3.18 mmol g^{-1}), 25 wt% (5.68 mmol g^{-1}), and 26 wt% (5.91 mmol g^{-1}) could be reached under open air / 500 ppm, 2 vol%, and 5 vol% CO_2, respectively. To the best of our knowledge, these are the highest capacities for CO_2 absorption by DESs and ILs under low concentrations of CO_2, *via* tuning the structures of AILs and the molar ratio of AIL to HBD. The spectroscopic investigations revealed that the anion-induced multi-site cooperations of O···CO_2 and N···CO_2 were the reason of ultrahigh CO_2 capacities. The possible mechanism of CO_2 capture by [DBNH][Pyrz]:EG (1:1) indicated that these reactions were initiated by [Pyrz] anions and resulted in two routes with three forms of absorbed CO_2, including two kinds of O···CO_2 carbonates ([EG − CO_2] and [CO_2 − EG − CO_2]$^{2-}$) and a kind of N···CO_2 carbamate ([Pyrz − CO_2]). Thermodynamic properties of CO_2 capture by [DBNH][Pyrz]:EG (1:1), such as the apparent chemical equilibrium constant (K'), the apparent change of molar Gibbs free energy of the reaction ($\Delta_r G'_m$), the apparent change of molar enthalpy of the reaction ($\Delta_r H'_m$), and the apparent change of molar entropy of the reaction ($\Delta_r S'_m$), were studied. The results indicated that $\Delta_r H'_m$ is more favorable than other thermodynamic properties for CO_2 capture under low concentration CO_2 through chemical absorption. We believe that the significant improvements made in this work on CO_2 capture over conventional sorbents provide an alternative strategy for industrial gas capture and utilization *via* anion-induced multi-site cooperations.

CRediT authorship contribution statement

Guokai Cui: Writing – review & editing, Writing – original draft, Supervision, Project administration, Investigation, Funding acquisition, Formal analysis, Conceptualization. **Yepin Cheng:** Visualization, Investigation, Data curation. **Wei Zhang:** Formal analysis. **Xiangyu Shen:** Validation, Formal analysis. **Lai Li:** Data curation. **Ruina Zhang:** Visualization, Methodology, Data curation. **Yaoji Chen:** Formal analysis. **Quanli Ke:** Funding acquisition, Formal analysis. **Chunliang Ge:** Formal analysis. **Huayan Liu:** Methodology, Formal analysis. **Wenyang Fan:** Resources, Formal analysis. **Hanfeng Lu:** Writing – review & editing, Supervision, Resources, Project administration, Funding acquisition, Formal analysis, Conceptualization.

Declaration of competing interest

The authors declare that they have no known competing financial interests or personal relationships that could have appeared to influence the work reported in this paper.

Acknowledgements

This work was supported by the National Natural Science Foundation of China (No. 22378353, No. 22078294), Key Research and Development Project in Zhejiang Province (No. 2024C03108, No. 2024C03114, No. 2023C03127), the Zhejiang Provincial Natural Science Foundation of China (No. LTGS24E080008), the Zhejiang Provincial Postdoctoral Science Foundation (No. ZJ2023145), and the Zhejiang Zheneng Technology & Environment Group Co., Ltd. "Research and Development of Technology and Equipment based on Ionic Liquids for Carbon Capture from Flue Gas with Low Energy Consumption" Technology Project (No. ZNKJ-2024-077).

Appendix A. Supplementary data

Supplementary data to this article can be found online at https://doi.org/10.1016/j.cej.2024.159193.

Data availability

Data will be made available on request.

References

[1] E.S. Sanz-Pérez, C.R. Murdock, S.A. Didas, C.W. Jones, Direct Capture of CO2 from Ambient Air, Chem. Rev. 116 (19) (2016) 11840–11876, https://doi.org/10.1021/acs.chemrev.6b00173.
[2] J.A. Rudd, Direct air capture: fledgling technology or world saviour? Nat. Rev. Chem. 7 (6) (2023) 377, https://doi.org/10.1038/s41570-023-00496-9.
[3] R.W. Baker, K. Lokhandwala, Natural Gas Processing with Membranes: An Overview, Ind. Eng. Chem. Res. 47 (7) (2008) 2109–2121, https://doi.org/10.1021/ie071083w.
[4] A. Mukhtar, S. Saqib, N.B. Mellon, M. Babar, S. Rafiq, S. Ullah, M.A. Bustam, A. G. Al-Sehemi, N. Muhammad, M. Chawla, CO2 capturing, thermo-kinetic principles, synthesis and amine functionalization of covalent organic polymers for CO2 separation from natural gas: A review, J. Nat. Gas Sci. Eng. 77 (2020) 103203, https://doi.org/10.1016/j.jngse.2020.103203.
[5] M.M. Mohd Pauzi, N. Azmi, K.K. Lau, Emerging Solvent Regeneration Technologies for CO2 Capture through Offshore Natural Gas Purification Processes, Sustainability 14 (7) (2022) 4350, https://doi.org/10.3390/su14074350.
[6] S. Faramawy, T. Zaki, A.A.E. Sakr, Natural gas origin, composition, and processing: A review, J. Nat. Gas Sci. Eng. 34 (2016) 34–54, https://doi.org/10.1016/j.jngse.2016.06.030.
[7] T. Zhao, X. Yang, Z. Tu, X. Hu, Efficient SO2 capture and conversion to cyclic sulfites by protic ionic liquid-based deep eutectic solvents under mild conditions, Sep. Purif. Technol. 318 (2023) 123981, https://doi.org/10.1016/j.seppur.2023.123981.
[8] G. Cui, J. Zheng, X. Luo, W. Lin, F. Ding, H. Li, C. Wang, Tuning Anion-Functionalized Ionic Liquids for Improved SO_2 Capture, Angew. Chem., Int. Ed. 52 (40) (2013) 10620-10624. https://doi.org/10.1002/anie.201305234.
[9] G. Cui, J. Liu, S. Lyu, H. Wang, Z. Li, R. Zhang, J. Wang, SO2 absorption in highly efficient chemical solvent AChBr + Gly compared with physical solvent ChBr + Gly, J. Mol. Liq. 330 (2021) 115650, https://doi.org/10.1016/j.molliq.2021.115650.
[10] L. Jiang, K. Mei, K. Chen, R. Dao, H. Li, C. Wang, Design and prediction for highly efficient SO2 capture from flue gas by imidazolium ionic liquids, Green Energy Environ. 7 (1) (2022) 130–136, https://doi.org/10.1016/j.gee.2020.08.008.
[11] S. Ren, Y. Hou, K. Zhang, W. Wu, Ionic liquids: Functionalization and absorption of SO_2, Green Energy Environ. 3 (3) (2018) 179–190, https://doi.org/10.1016/j.gee.2017.11.003.
[12] R. Zhai, X. He, K. Mei, K. Chen, N. Cao, W. Lin, H. Li, C. Wang, Ultrahigh Nitric Oxide Capture by Tetrakis(azolyl)borate Ionic Liquid through Multiple-Sites Uniform Interaction, ACS Sustainable Chem. Eng. 9 (8) (2021) 3357–3362, https://doi.org/10.1021/acssuschemeng.1c00024.
[13] K. Chen, G. Shi, X. Zhou, H. Li, C. Wang, Highly Efficient Nitric Oxide Capture by Azole-Based Ionic Liquids through Multiple-Site Absorption, Angew. Chem., Int. Ed. 55(46) (2016) 14364-14368. https://doi.org/10.1002/anie.201607528.
[14] Y. Sun, M. Gao, S. Ren, Q. Zhang, Y. Hou, W. Wu, Highly Efficient Absorption of NO by Amine-Based Functional Deep Eutectic Solvents, Energy Fuels 34 (1) (2020) 690–697, https://doi.org/10.1021/acs.energyfuels.9b03335.
[15] K. Li, K. Zong, X. Wang, G. Cui, D. Deng, Ionic liquids and deep eutectic solvents for NH3 absorption and separation: a review, New J. Chem. 47 (46) (2023) 21426–21445, https://doi.org/10.1039/D3NJ04455F.
[16] X. Sun, G. Li, S. Zeng, L. Yuan, L. Bai, X. Zhang, Ultra-high NH3 absorption by triazole cation-functionalized ionic liquids through multiple hydrogen bonding, Sep. Purif. Technol. 307 (2023) 122825, https://doi.org/10.1016/j.seppur.2022.122825.
[17] R. Qiu, X. Luo, L. Yang, J. Li, X. Chen, C. Peng, J. Lin, Regulated Threshold Pressure of Reversibly Sigmoidal NH3 Absorption Isotherm with Ionic Liquids, ACS Sustainable Chem. Eng. 8 (3) (2020) 1637–1643, https://doi.org/10.1021/acssuschemeng.9b06555.
[18] G. Cui, K. Jiang, H. Liu, Y. Zhou, Z. Zhang, R. Zhang, H. Lu, Highly efficient CO removal by active cuprous-based ternary deep eutectic solvents [HDEEA][Cl] + CuCl + EG, Sep. Purif. Technol. 274 (2021) 118985, https://doi.org/10.1016/j.seppur.2021.118985.
[19] D.-J. Tao, X.-C. An, Z.-T. Gao, Z.-M. Li, Y. Zhou, Cuprous-based composite ionic liquids for the selective absorption of CO: Experimental study and thermodynamic analysis, AIChE J. 68 (5) (2022) e17631, https://doi.org/10.1002/aic.17631.
[20] L. Peng, M. Shi, Y. Pan, Z. Tu, X. Hu, X. Zhang, Y. Wu, Ultrahigh carbon monoxide capture by novel protic cuprous-functionalized dicationic ionic liquids through complexation interactions, Chem. Eng. J. 451 (2023) 138519, https://doi.org/10.1016/j.cej.2022.138519.
[21] Y. Xu, R. Zhang, Y. Zhou, D. Hu, C. Ge, W. Fan, B. Chen, Y. Chen, W. Zhang, H. Liu, G. Cui, H. Lu, Tuning ionic liquid-based functional deep eutectic solvents and other functional mixtures for CO_2 capture, Chem. Eng. J. 463 (2023) 142298, https://doi.org/10.1016/j.cej.2023.142298.
[22] X. Suo, Y. Fu, C.-L. Do-Thanh, L.-Q. Qiu, D.-E. Jiang, S.M. Mahurin, Z. Yang, S. Dai, CO_2 Chemisorption Behavior in Conjugated Carbanion-Derived Ionic Liquids via Carboxylic Acid Formation, J. Am. Chem. Soc. 144 (47) (2022) 21658–21663, https://doi.org/10.1021/jacs.2c09189.
[23] K. Wang, Z. Zhang, S. Wang, L. Jiang, H. Li, C. Wang, Dual-Tuning Azole-Based Ionic Liquids for Reversible CO2 Capture from Ambient Air, ChemSusChem 17 (16) (2024) e202301951, https://doi.org/10.1002/cssc.202301951.
[24] M. Chen, W. Xiong, W. Chen, S. Li, F. Zhang, Y. Wu, Synergy of carbanion siting and hydrogen bonding in super-nucleophilic deep eutectic solvents for efficient CO_2 capture, AIChE J. 70 (4) (2024) e18319, https://doi.org/10.1002/aic.18319.
[25] F.-F. Chen, K. Huang, Y. Zhou, Z.-Q. Tian, X. Zhu, D.-J. Tao, D.-e. Jiang, S. Dai, Multi-Molar Absorption of CO_2 by the Activation of Carboxylate Groups in Amino Acid Ionic Liquids, Angew. Chem., Int. Ed. 55(25) (2016) 7166-7170. https://doi.org/10.1002/anie.201602919.
[26] B. Yoon, S. Chen, G.A. Voth, On the Key Influence of Amino Acid Ionic Liquid Anions on CO_2 Capture, J. Am. Chem. Soc. 146 (2) (2024) 1612–1618, https://doi.org/10.1021/jacs.3c11808.
[27] G. Cui, J. Wang, S. Zhang, Active chemisorption sites in functionalized ionic liquids for carbon capture, Chem. Soc. Rev. 45 (15) (2016) 4307–4339, https://doi.org/10.1039/C5CS00462D.
[28] R. Zhang, Q. Ke, Z. Zhang, B. Zhou, G. Cui, H. Lu, Tuning Functionalized Ionic Liquids for CO_2 Capture, Int. J. Mol. Sci. 23 (19) (2022) 11401, https://doi.org/10.3390/ijms231911401.
[29] S. Zeng, X. Zhang, L. Bai, X. Zhang, H. Wang, J. Wang, D. Bao, M. Li, X. Liu, S. Zhang, Ionic-Liquid-Based CO_2 Capture Systems: Structure, Interaction and Process, Chem. Rev. 117 (14) (2017) 9625–9673, https://doi.org/10.1021/acs.chemrev.7b00072.
[30] N. Gao, Y. Yang, Z. Wang, X. Guo, S. Jiang, J. Li, Y. Hu, Z. Liu, C. Xu, Viscosity of Ionic Liquids: Theories and Models, Chem. Rev. 124 (1) (2024) 27–123, https://doi.org/10.1021/acs.chemrev.3c00339.
[31] Y. Fu, X. Suo, Z. Yang, S. Dai, D.-E. Jiang, Computational Insights into Malononitrile-Based Carbanions for CO2 Capture, J. Phys. Chem. B 126 (36) (2022) 6979–6984, https://doi.org/10.1021/acs.jpcb.2c03082.
[32] S. Li, C. Zhao, C. Sun, Y. Shi, W. Li, Reaction Mechanism and Kinetics Study of CO2 Absorption into [C2OHmim][Lys], Energy Fuels 30 (10) (2016) 8535–8544, https://doi.org/10.1021/acs.energyfuels.6b01773.
[33] B.B. Hansen, S. Spittle, B. Chen, D. Poe, Y. Zhang, J.M. Klein, A. Horton, L. Adhikari, T. Zelovich, B.W. Doherty, B. Gurkan, E.J. Maginn, A. Ragauskas, M. Dadmun, T.A. Zawodzinski, G.A. Baker, M.E. Tuckerman, R.F. Savinell, J. R. Sangoro, Deep Eutectic Solvents: A Review of Fundamentals and Applications, Chem. Rev. 121 (3) (2021) 1232–1285, https://doi.org/10.1021/acs.chemrev.0c00385.
[34] X. Zhang, W. Xiong, L. Peng, Y. Wu, X. Hu, Highly selective absorption separation of H2S and CO2 from CH4 by novel azole-based protic ionic liquids, AIChE J. 66 (6) (2020) e16936, https://doi.org/10.1002/aic.16936.
[35] S. Wen, L. Zheng, X. Zhang, Y. Wu, Unveiling protic amino acid ionic liquids for the efficient capture of carbon dioxide, Chem. Commun. 60 (50) (2024) 6443–6446, https://doi.org/10.1039/D4CC01596G.
[36] Y. Liu, Z. Dai, Z. Zhang, S. Zeng, F. Li, X. Zhang, Y. Nie, L. Zhang, S. Zhang, X. Ji, Ionic liquids/deep eutectic solvents for CO2 capture: Reviewing and evaluating, Green Energy Environ. 6 (3) (2021) 314–328, https://doi.org/10.1016/j.gee.2020.11.024.
[37] L. Cao, J. Huang, X. Zhang, S. Zhang, J. Gao, S. Zeng, Imidazole tailored deep eutectic solvents for CO2 capture enhanced by hydrogen bonds, Phys. Chem. Chem. Phys. 17 (41) (2015) 27306–27316, https://doi.org/10.1039/C5CP04050G.
[38] Y. Gu, Y. Hou, S. Ren, Y. Sun, W. Wu, Hydrophobic Functional Deep Eutectic Solvents Used for Efficient and Reversible Capture of CO2, ACS Omega 5 (12) (2020) 6809–6816, https://doi.org/10.1021/acsomega.0c00150.
[39] G. Cui, N. Zhao, J. Wang, C. Wang, Computer-Assisted Design of Imidazolate-Based Ionic Liquids for Improving Sulfur Dioxide Capture, Carbon Dioxide Capture, and

Sulfur Dioxide/Carbon Dioxide Selectivity, Chem. Asian J. 12 (21) (2017) 2863–2872, https://doi.org/10.1002/asia.201701215.
[40] C. Wang, X. Luo, H. Luo, D.-e. Jiang, H. Li, S. Dai, Tuning the Basicity of Ionic Liquids for Equimolar CO_2 Capture, Angew. Chem., Int. Ed. 50(21) (2011) 4918-4922. https://doi.org/10.1002/anie.201008151.
[41] G. Shi, R. Zhai, H. Li, C. Wang, Highly efficient synthesis of alkylidene cyclic carbonates from low concentration CO2 using hydroxyl and azolate dual functionalized ionic liquids, Green Chem. 23 (1) (2021) 592–596, https://doi.org/10.1039/D0GC03510F.
[42] P. Goodrich, H.Q.N. Gunaratne, J. Jacquemin, L. Jin, Y. Lei, K.R. Seddon, Sustainable Cyclic Carbonate Production, Utilizing Carbon Dioxide and Azolate Ionic Liquids, ACS Sustainable Chem. Eng. 5 (7) (2017) 5635–5641, https://doi.org/10.1021/acssuschemeng.7b00355.
[43] G. Cui, M. Lv, D. Yang, Efficient CO2 absorption by azolide-based deep eutectic solvents, Chem. Commun. 55 (10) (2019) 1426–1429, https://doi.org/10.1039/C8CC10085C.
[44] H. Sang, L. Su, W. Han, F. Si, W. Yue, X. Zhou, Z. Peng, H. Fu, Basicity-controlled DBN-based deep eutectic solvents for efficient carbon dioxide capture, J. CO2 Util. 65 (2022) 102201, https://doi.org/10.1016/j.jcou.2022.102201.
[45] B. Jiang, C. Zhang, Q. Zhou, L. Zhang, J. Li, X. Tantai, Y. Sun, L. Zhang, Investigation of Efficient and Reversible CO2 Capture Using 1,5-Diazabicyclo [4.3.0]non-5-ene-Based Quasi-Deep Eutectic Solvents, ACS Sustainable Chem. Eng. 12(37) (2024) 14109-14118. https://doi.org/10.1021/acssuschemeng.4c05906.
[46] J. Ruan, X. Ye, R. Wang, L. Chen, L. Deng, Z. Qi, Experimental and theoretical study on efficient CO2 absorption coordinated by molecules and ions of DBN and 1,2,4-triazole formed deep eutectic solvents, Fuel 334 (2023) 126709, https://doi.org/10.1016/j.fuel.2022.126709.
[47] W. Yue, W. Han, M. Yuan, X. Zhou, H. Fu, Three-component CO2 binding organic liquids for efficient and reversible CO2 capture: Effect of molar ratio of component on mechanism, J. Mol. Liq. 399 (2024) 124400, https://doi.org/10.1016/j.molliq.2024.124400.
[48] S. Sarmad, Y. Xie, J.-P. Mikkola, X. Ji, Screening of deep eutectic solvents (DESs) as green CO2 sorbents: from solubility to viscosity, New J. Chem. 41 (1) (2017) 290–301, https://doi.org/10.1039/C6NJ03140D.
[49] A. Li, Z. Tian, T. Yan, D.-E. Jiang, S. Dai, Anion-Functionalized Task-Specific Ionic Liquids: Molecular Origin of Change in Viscosity upon CO2 Capture, J. Phys. Chem. B 118 (51) (2014) 14880–14887, https://doi.org/10.1021/jp5100236.
[50] X.Y. Luo, X. Fan, G.L. Shi, H.R. Li, C.M. Wang, Decreasing the Viscosity in CO_2 Capture by Amino-Functionalized Ionic Liquids through the Formation of Intramolecular Hydrogen Bond, J. Phys. Chem. B 120 (10) (2016) 2807–2813, https://doi.org/10.1021/acs.jpcb.5b10553.
[51] S. Ren, Y. Hou, S. Tian, X. Chen, W. Wu, What Are Functional Ionic Liquids for the Absorption of Acidic Gases? J. Phys. Chem. B 117 (8) (2013) 2482–2486, https://doi.org/10.1021/jp311707e.
[52] W.M.O., State of the global climate, (WMO-No. 1316), World Meteorological Organization, Geneva 2, Switzerland 2023 (2022) 3–5. https://library.wmo.int/records/item/66214-state-of-the-global-climate-2022.
[53] Z. Liu, S. Shi, Y. Ji, K. Wang, T. Tan, J. Nielsen, Opportunities of CO2-based biorefineries for production of fuels and chemicals, Green Carbon 1 (1) (2023) 75–84, https://doi.org/10.1016/j.greenca.2023.09.002.
[54] X. Zhu, W. Xie, J. Wu, Y. Miao, C. Xiang, C. Chen, B. Ge, Z. Gan, F. Yang, M. Zhang, D. O'Hare, J. Li, T. Ge, R. Wang, Recent advances in direct air capture by adsorption, Chem. Soc. Rev. 51 (15) (2022) 6574–6651, https://doi.org/10.1039/D1CS00970B.
[55] Z. Yang, S. Dai, Challenges in engineering the structure of ionic liquids towards direct air capture of CO2, Green Chem. Eng. 2 (4) (2021) 342–345, https://doi.org/10.1016/j.gce.2021.08.003.
[56] S.P. Teong, Y. Zhang, Direct capture and separation of CO2 from air, Green Energy Environ. 9 (3) (2024) 413–416, https://doi.org/10.1016/j.gee.2023.06.005.
[57] N. Zhang, Z. Huang, H. Zhang, J. Ma, B. Jiang, L. Zhang, Highly Efficient and Reversible CO2 Capture by Task-Specific Deep Eutectic Solvents, Ind. Eng. Chem. Res. 58 (29) (2019) 13321–13329, https://doi.org/10.1021/acs.iecr.9b02041.
[58] N. Ahmad, X. Lin, X. Wang, J. Xu, X. Xu, Understanding the CO2 capture performance by MDEA-based deep eutectics solvents with excellent cyclic capacity, Fuel 293 (2021) 120466, https://doi.org/10.1016/j.fuel.2021.120466.
[59] Y. Bi, Z. Hu, X. Lin, N. Ahmad, J. Xu, X. Xu, Efficient CO2 capture by a novel deep eutectic solvent through facile, one-pot synthesis with low energy consumption and feasible regeneration, Sci. Total Environ. 705 (2020) 135798, https://doi.org/10.1016/j.scitotenv.2019.135798.
[60] Z. Li, L. Wang, C. Li, Y. Cui, S. Li, G. Yang, Y. Shen, Absorption of Carbon Dioxide Using Ethanolamine-Based Deep Eutectic Solvents, ACS Sustainable Chem. Eng. 7 (12) (2019) 10403–10414, https://doi.org/10.1021/acssuschemeng.9b00555.
[61] Z. Wang, Z. Wang, J. Chen, C. Wu, D. Yang, The Influence of Hydrogen Bond Donors on the CO2 Absorption Mechanism by the Bio-Phenol-Based Deep Eutectic Solvents, Molecules 26 (23) (2021) 7167, https://doi.org/10.3390/molecules26237167.
[62] Z. Wang, Z. Wang, X. Huang, D. Yang, C. Wu, J. Chen, Deep eutectic solvents composed of bio-phenol-derived superbase ionic liquids and ethylene glycol for CO_2 capture, Chem. Commun. 58 (13) (2022) 2160–2163, https://doi.org/10.1039/D1CC06856C.
[63] C. Mukesh, S.G. Khokarale, P. Virtanen, J.-P. Mikkola, Rapid desorption of CO2 from deep eutectic solvents based on polyamines at lower temperatures: an alternative technology with industrial potential, Sustain. Energy Fuels 3 (8) (2019) 2125–2134, https://doi.org/10.1039/C9SE00112C.
[64] Y.-Y. Lee, D. Penley, A. Klemm, W. Dean, B. Gurkan, Deep Eutectic Solvent Formed by Imidazolium Cyanopyrrolide and Ethylene Glycol for Reactive CO_2 Separations, ACS Sustainable Chem. Eng. 9 (3) (2021) 1090–1098, https://doi.org/10.1021/acssuschemeng.0c07217.
[65] F.-F. Chen, K. Huang, J.-P. Fan, D.-J. Tao, Chemical solvent in chemical solvent: A class of hybrid materials for effective capture of CO2, AIChE J. 64 (2) (2018) 632–639, https://doi.org/10.1002/aic.15952.
[66] C. Li, T. Zhao, A. Yang, F. Liu, Highly Efficient Absorption of CO2 by Protic Ionic Liquids-Amine Blends at High Temperatures, ACS Omega 6 (49) (2021) 34027–34034, https://doi.org/10.1021/acsomega.1c05416.
[67] C. Wang, H. Luo, D.-e. Jiang, H. Li, S. Dai, Carbon Dioxide Capture by Superbase-Derived Protic Ionic Liquids, Angew. Chem., Int. Ed. 49(34) (2010) 5978-5981. https://doi.org/10.1002/anie.201002641.
[68] X. Luo, Y. Guo, F. Ding, H. Zhao, G. Cui, H. Li, C. Wang, Significant Improvements in CO_2 Capture by Pyridine-Containing Anion-Functionalized Ionic Liquids through Multiple-Site Cooperative Interactions, Angew. Chem., Int. Ed. 53(27) (2014) 7053-7057. https://doi.org/10.1002/anie.201400957.
[69] Y. Huang, G. Cui, Y. Zhao, H. Wang, Z. Li, S. Dai, J. Wang, Preorganization and Cooperation for Highly Efficient and Reversible Capture of Low-Concentration CO_2 by Ionic Liquids, Angew. Chem., Int. Ed. 56(43) (2017) 13293-13297. https://doi.org/10.1002/anie.201706280.
[70] S. Wen, T. Wang, X. Zhang, W. Xu, X. Hu, Y. Wu, Novel amino acid ionic liquids prepared via one-step lactam hydrolysis for the highly efficient capture of CO_2, AIChE J. 69 (11) (2023) e18206, https://doi.org/10.1002/aic.18206.
[71] X. Sun, S. Zeng, G. Li, Y. Bai, M. Shang, J. Zhang, X. Zhang, Selective CO2 separation through physicochemical absorption by triazole-functionalized ionic liquid binary absorbents, AIChE J. 70 (5) (2024) e18376, https://doi.org/10.1002/aic.18376.
[72] X. Suo, Z. Yang, Y. Fu, C.-L. Do-Thanh, H. Chen, H. Luo, D.-E. Jiang, S.M. Mahurin, H. Xing, S. Dai, CO_2 Chemisorption Behavior of Coordination-Derived Phenolate Sorbents, ChemSusChem 14 (14) (2021) 2854–2859, https://doi.org/10.1002/cssc.202100666.
[73] D. Xiong, G. Cui, J. Wang, H. Wang, Z. Li, K. Yao, S. Zhang, Reversible Hydrophobic–Hydrophilic Transition of Ionic Liquids Driven by Carbon Dioxide, Angew. Chem., Int. Ed. 54(25) (2015) 7265-7269. https://doi.org/10.1002/anie.201500695.
[74] X. Li, H. Li, Z. Ling, D. Xu, T. You, Y.-Y. Wu, F. Xu, Room-Temperature Superbase-Derived Ionic Liquids with Facile Synthesis and Low Viscosity: Powerful Solvents for Cellulose Dissolution by Destroying the Cellulose Aggregate Structure, Macromolecules 53 (9) (2020) 3284–3295, https://doi.org/10.1021/acs.macromol.0c00592.
[75] W. Qian, Y. Xu, B. Xie, Y. Ge, H. Shu, Alkanolamine-based dual functional ionic liquids with multidentate cation coordination and pyrazolide anion for highly efficient CO2 capture at relatively high temperature, Int. J. Greenhouse Gas Control 56 (2017) 194–201, https://doi.org/10.1016/j.ijggc.2016.11.032.
[76] G. Zerbi, C. Alberti, Infrared spectra of pyrazoles—I: Pyrazoles mono-alkyl substituted, Spectrochim. Acta 18 (3) (1962) 407–423, https://doi.org/10.1016/S0371-1951(62)80149-0.
[77] G. Giubertoni, O.O. Sofronov, H.J. Bakker, Effect of intramolecular hydrogen-bond formation on the molecular conformation of amino acids, Communications Chemistry 3 (1) (2020) 84, https://doi.org/10.1038/s42004-020-0329-7.
[78] Y. Guo, T. Chen, Y. Xu, Carboxylative cyclization of atmospheric CO2 with alkynol catalyzed by a 1-methylhydantoin anion-functionalized ionic liquid via chelative interactions, Chem. Commun. 60 (95) (2024) 14089–14092, https://doi.org/10.1039/D4CC03586K.
[79] Y. Huang, G. Cui, H. Wang, Z. Li, J. Wang, Tuning ionic liquids with imide-based anions for highly efficient CO_2 capture through enhanced cooperations, J. CO2 Util. 28 (2018) 299–305, https://doi.org/10.1016/j.jcou.2018.10.013.
[80] Y. Huang, G. Cui, Y. Zhao, H. Wang, Z. Li, S. Dai, J. Wang, Reply to the Correspondence on "Preorganization and Cooperation for Highly Efficient and Reversible Capture of Low-Concentration CO_2 by Ionic Liquids", Angew. Chem., Int. Ed. 58(2) (2019) 386-389. https://doi.org/10.1002/anie.201808486.
[81] H. Fu, Y. Hou, H. Sang, T. Mu, X. Lin, Z. Peng, P. Li, J. Liu, Carbon dioxide capture by new DBU-based DES: The relationship between ionicity and absorptive capacity, AIChE J. 67 (7) (2021) e17244, https://doi.org/10.1002/aic.17244.
[82] G. Cui, Y. Xu, D. Hu, Y. Zhou, C. Ge, H. Liu, W. Fan, Z. Zhang, B. Chen, Q. Ke, Y. Chen, B. Zhou, W. Zhang, R. Zhang, H. Lu, Tuning functional ionic deep eutectic solvents as green sorbents and catalysts for highly efficient capture and transformation of CO_2 to quinazoline-2,4(1*H*,3*H*)-dione and its derivatives, Chem. Eng. J. 469 (2023) 143991, https://doi.org/10.1016/j.cej.2023.143991.
[83] R. Li, B. Zhang, N. Hou, C. Li, J. Xie, J. He, X. Chen, Q. Xu, J. Zhao, D. Han, The solubility profile and apparent thermodynamic analysis of doxofylline in pure and mixed solvents, J. Chem. Thermodyn. 148 (2020) 106126, https://doi.org/10.1016/j.jct.2020.106126.